DOI: https://doi.org/10.57233/ijsgs.v10i2.664 ISSNp: 2488-9229; ISSNe: 3027-1118

IJSGS FUGUSAU VOL10 (2) WEBSITE: https://fugus-ijsgs.com.ng

INTERNATIONAL JOURNAL OF SCIENCE FOR GLOBAL SUSTAINABILITY

(A PUBLICATION OF FACULTY OF SCIENCE, FEDERAL UNIVERSITY GUSAU, NIGERIA)

Experimental Analysis of the Effect of Shear Forces on Oil-Water Separation, Using a High Shear Mixer

***Ridwan Muhammad Mahmood[1] and Nuru Garba Lame[2]**

[1]Department of Applied Geophysics, Federal University Birnin Kebbi

[2]Department of Material Management, Geo-Derrick Nigeria Limited

***Correspondence Authors' Email**: mr.mahmood@fubk.edu.ng

Received on: April, 2024 **Revised and Accepted on:** May, 2024 **Published on:** July, 2024

ABSTRACT

In most water-drive reservoirs, the dispersion of oil in produced water is a result of high water cut conditions. During production, the oil droplet size decreases as a result of their encounter with process facilities such as: valves and pumps which has a detrimental impact on upstream separation. The present work performed an experimental analysis of the factors affecting the formation of droplets. Laboratory mixing of oil and water was conducted using a high-shear mixer. An analysis of the droplet size distribution of three different oil viscosities were obtained using a microscopic technique. The overall results show that the coalescence rate decreases with increasing oil viscosity and the rate of agitation. Droplet sizes within the range of 3 – 100 micrometers were observed. The results obtained from this experiment can be used to test the design of new separators and can provide an avenue for the design of low shear centrifugal pumps.

Keywords: Droplet size, Shear rate, Viscosity, Emulsion, Separators

1.0 INTRODUCTION

In most water drive reservoirs, the volume of produced water can be significantly higher than oil production in some oil fields, and the amount of water produced from a reservoir increases with the age of the field (Liu, 2021). The produced water containing some amount of dispersed oil, dissolved oil, solids, and chemical residues together with emulsifying agents present in the reservoir tends to form a very tight emulsion. For economic and environmental concerns, the produced water is cleaned into a number of treatment stages to reduce the oil content to an acceptable level. This water is either injected into the reservoir to enhance hydrocarbon recovery or discharged overboard (Walsh, 2016).

To separate the different phases (i.e. oil, water, and gas) into clean phases, large gravity base separators are used in a production platform. The most common process system, where the oil, gas, and water are separated, has 2 to 4 separation and produced water treatment stages (Walsh, 2016). In between the different separators and produced water treatment stages, valves, and pumps are installed to control flow and pressure. These valves and pumps are considered as a necessary evil with regards to the separation efficiency (Walsh, 2016). Shear forces acting on the fluids passing through the valves and pumps cause further emulsification and droplet break up, which have a detrimental impact on the efficiency of the upstream separator. Tight emulsions can cause several operational challenges such as plant and equipment instability, increased consumption of emulsion breakers, off-spec crude production, and high-pressure drops in flow lines (Goodarzi and Zendehboudi, 2019). A number of measures can be employed to counteract the negative impact on separation efficiency from these valves and pumps. The residence time of a separator can be increased, more treatment stages can be utilized, heat can be applied, separation-enhancing production chemicals can be utilized, etc. These measures can, however, have a significant negative impact such as increased footprint, weight, power, and chemical consumption. Therefore, a more constructive way is to find a solution to mitigate the cause of the problem, and this can only be achieved by the design and construction of low-shear production facilities (Walsh, 2016).

One of the most important design parameters to determine the efficiency of an oil-water separator is the droplet size analysis. This is a powerful tool for determining the size of a separator and can also be used to define low-shear characteristics of many process facilities, such as: pumps, pressure-reducing valves, atomizers, and hydro-cyclones. In recent years, many advances have been made to analyze the size distribution of dispersed oil droplets for various industrial applications such as food and drinks, pharmaceuticals and cosmetics, and many more emulsion-based products. However, very few researches are available about the droplet size in the production stream due to the difficulty of measuring the droplet size of hydrocarbons in water emulsion (Dhandhi *et al.*, 2022).

The present work is part of an ongoing research project for the design and construction of a high-capacity plate

separator, at the Centre for Flow Measurement and Fluid Dynamics (FMFM), Coventry University, United Kingdom. The main objective of this research focuses on the application of experimental techniques to investigate the factors affecting the breakup and coalescence of droplets in oil-water emulsions, practically and theoretically using the relevant mathematical equations.

1.1 Justification of the study

For economic reasons, the most widely used pumping device in the oil industry is the centrifugal pump, and studies have shown that the rotational speed of this type of pump has a very high negative effect on the droplet size distribution with decreasing the rotational speed increases the size of droplets (Al-Kayiem *et al.,* 2022). This kind of problem is of great concern to the industry, and very few researches are presently available in the literature regarding the effect of shear on separation efficiency and other operational challenges on flow systems. The knowledge of fluid behavior under the presence of shear forces can help to make sound process decisions for the optimal operation of oil production.

Al-kayiem *et al.,* (2022), analyzed the mean droplet size at pump outlets for different types of pumps over a range of heads. The measurement was performed in an actual production stream to determine the effect of pump shear on oil droplet diameter. The results of his work provide the basis for decision-making in selecting an optimum oil-water treatment facility.

To correlate droplet size with physical parameters, and conditions of emulsions, inorder to improve the separation efficiency of separators based on the gravity settling method. The present work deals with a laboratory-scale mixing of oil and water using a Basic Ultra Turrax high-shear mixer (T 18/10). This device has the same working principle as that of a centrifugal pump. Varying the rotor speed of this device helps to analyze the effect of shear force and viscosity on the breakup and coalescence of oil droplets.

The work of Mutsch *et al.,* (2021), neither considers oil viscosity nor the concentration of the dispersed phase, and the subsequent research by Dong *et, al* (2022), investigated the effect of viscosity on the size distribution of droplets by changing the volumetric fraction of the dispersed phase (oil). Al-kayiem *et al.,* (2022), experiments also obtained results by altering the temperature of the homogeneous mixture of oil and water. However, the size distribution of droplets is characterized by the nature of the emulsion (hydrocarbons in water). Studies have shown that a higher viscous oil in water causes a very tight emulsion. The tighter the emulsion, the higher the rate of coalescence. Hence, it is essential to analyze droplet size based on oil type. In view of the above, the present experiment used different oil types, with viscosities ranging from medium to extra heavy.

2.0 METHODOLOGY

This chapter describes the procedures and techniques applied, the system properties, data analysis, practical limitations as well as the measures that were taken for investigating the aforementioned aims and objectives.

2.1 Droplet Size Measuring Techniques

Various techniques have been developed to obtain particle size data, and each particle sizing technique is based on a particular physical principle of the system (Hinze, 1995). Some of these techniques include:

2.1.1 Laser Diffraction Technique

This is the most widely used industrial particle sizing technique, which is based on the principle for scattering of light and the knowledge of the optical properties of the material. It is a volume-based technique, used to report a volume equivalent spherical diameter of the irregularly shaped particles. An example of this is the Malvern instruments, which have been used for diluting oil-water dispersions and annular gas–water flow (Liu, 2021).

2.1.2 Sieve Analysis or Gradation Test

This technique is mainly used in analyzing and classifying the size of powdered particles. The particle size distribution depends on the size of the mesh. This technique is usually applied in the preparations of foodstuffs and pharmaceutical products (Allen, 2003).

2.1.3 Sedimentation Technique

This technique measures the size of a particle based on the rate of sedimentation. It gives the equivalent spherical diameter of irregular-shaped particles, having the same sedimentation rate. The technique is mostly used to determine the relationship between settling velocity and the size of a particle (especially solid). One of the limitations of this technique is that inaccurate data is usually generated due to the effects of convection, Brownian motion, and thermal diffusion (Allen, 2003).

2.1.4 Microscopic Technique or Image Analysis

This involves visual inspection of particles to estimate the average size of the specimen. An embedded ruler, known as the ocular micrometer, which is embedded in one of the eyepieces is used to obtain the average size (in diameter) of the particle, depending on the degree of magnification.

An advantage of the majority of the techniques that have been employed is that the droplet size distribution is measured directly or can be obtained by simple analysis.

DOI: https://doi.org/10.57233/ijsgs.v10i2.664 ISSNp: 2488-9229; ISSNe: 3027-1118
IJSGS FUGUSAU VOL10 (2) WEBSITE: https://fugus-ijsgs.com.ng

However, these methods can only obtain useful data from dilute systems.

Thus, considering the nature of the homogenous mixture (very tight emulsion) and the particle size range (between 2 and 150 microns), the present work uses the microscopic technique to obtain reliable and accurate droplet size data. The advantage of this technique is that it offers a direct view of the dispersed droplets. A similar technique was employed by (Eggers *et al.,* 2008), when they studied the shape and size distributions of particles in 2 dimensions, based on the microscopic picture of particles in suspension. Similarly, an automatic image analysis of droplet size distribution was obtained by (Lebaz *et al.,* 2021). But this time, a high-precision light microscope (Olympus CX 31) was used, to determine the average sizes of the dispersed oil droplets in oil-water emulsion at various realistic shear rates.

2.2 Experimental Procedure

At the environmental science laboratory, science and health building, Coventry University. An experimental setup was arranged to determine the average droplet size of oil-water emulsion. 30 batches of 50 ml beakers were prepared, each batch contained a volume of 40 ml of distilled water and oil in the ratio of 7:3, (12 ml of Pennine gear oil and 28 ml of distilled water). The volumetric ratio (7:3) was maintained throughout the experiment. Even though some researchers have proved that dispersed phase concentration has an effect on the size distribution of droplets in an emulsion. Other research has shown that the effect is insignificant. Goodazi and Zendehboudi (2019), characterizes dispersion and emulsification in continuous in-line mixers and they discovered that over a range of dispersed phase concentrations studied, drop size was independent of the volume percentage of the dispersed phase. Likewise, for a batch mixer, Gallasi *et al.*, (2011), discovered that the impact of the dispersed phase volume fraction on the droplet size is not significant. Therefore, the effect of dispersed phase volumetric fraction was not considered in the present work.

The rotor (suction head) of the shear mixer was placed in the batch beaker and the rotational speed was slowly adjusted to the desired speed. Each sample was vigorously agitated (dispersed) at a desired set point (of speed) for 60s.

Each time a sample was prepared, a portion of the sample was quickly placed on the microscopic slide, using a disposable pipette, and suitable calibration images were collected to determine the average size of dispersed oil droplets for each sample. The observation was made using the X10, X20, and X40 objectives of the microscope. A paper towel was used to wipe away the residual emulsion and the apparatus was also cleaned, between experiments with detergent (Decon 90) and water. To ensure that an accurate result was obtained, the procedure was repeated twice for each sample.

Figure 1: Dispersion of Oil in Water Using High Shear Mixer (Basic Ultra Turrax T 10/18).

Figure 2: Microscopic Droplet Size Analysis Using A High Precision Light Microscope (Olympus CX 31)

2.3 Experimental Limitations and Measures

An open beaker was used. Air bubbles may be present because the available equipment does not have a provision for a close system emulsification process. A significant amount of time was consumed by the technique employed. Also, the resolution limit on the microscope contributed to some minor errors, when analyzing an emulsion with different magnifications. Therefore, Kohler illumination was ensured. The microscopic coverslip was not used, to avoid squashing the droplet. Making them appear larger than their actual size.

2.4 Droplet Size Interpretation Techniques

DOI: https://doi.org/10.57233/ijsgs.v10i2.664 ISSNp: 2488-9229; ISSNe: 3027-1118

The most widely used distribution functions to determine the size of droplets in a sample are normal, log-normal, and Rosin-Rammler distributions.

2.4.1 Normal Distribution

In the normal distribution, a number distribution function may be used to determine the number of droplets of diameter D, as

$$f(D) = \frac{1}{\sqrt{2\pi}s_n} \exp\left[-\frac{1}{2s_n^2}(D - D^*)^2\right] \quad (1)$$

where s_n is the standard deviation, a measure of the deviation of values of D from the mean value, and s_n^2 is the variance. A plot of the distribution function is called a standard normal distribution curve, where the area under the curve from - ∞ to + ∞ is equal to 1 (Liu, 2021). The cumulative standard number distribution function is the integral of the standard normal distribution function as:

$$f(D) = \frac{1}{\sqrt{2\pi}s_n} \int_{-\infty}^{D} exp\left[-\frac{1}{2s_n^2}(D - D^*)^2\right] d(D - D^*/s_n)^2 \quad (2)$$

2.4.2 Log-Normal Distribution

The Log-Normal distribution is obtained by the substitution of the "variable" in a normal distribution by the "log of the variable". Then log-normal distribution function becomes:

$$f(D) = \frac{\Delta N}{\Delta D} = \frac{1}{\sqrt{2\pi}Ds_g} \exp\left[-\frac{1}{2s_g^2}\left(lnD - lnD_{ng}{}^*\right)^2\right] \quad (3)$$

where $D_{ng}{}^*$ denotes the number geometric mean droplet diameter and s_g is the geometric standard deviation. Plotting droplet size data on a log-probability graph paper will generate a straight line if the data follow a log-normal distribution (Liu, 2021).

$$f(D^2) = \frac{\Delta N}{\Delta D} = \frac{1}{\sqrt{2\pi}Ds_g} \exp 2\left[-\frac{1}{2s_g^2}\left(lnD - lnD_{ng}{}^*\right)^2\right] \quad (4)$$

$$f(D^3) = \frac{\Delta N}{\Delta D} = \frac{1}{\sqrt{2\pi}Ds_g} \exp 3\left[-\frac{1}{2s_g^2}\left(lnD - lnD_{ng}{}^*\right)^2\right] \quad (5)$$

Equations 4 and 5 describe the log-normal distribution functions based on surface and volume, respectively.

2.4.3 Rosin-Rammler Distribution

This distribution is defined as a cumulative distribution function only, not having a probability density function. The advantage of this distribution is its ease of use. Rosin-Rammler distribution is given as:

$$V = 1 - \exp\left[-\left(\frac{D}{D^*}\right)^q\right] \quad (6)$$

where V is the fraction of the total volume of droplets smaller than D, D^* is the particle size at 63.2% (finesse number) and q is the uniform index (Liu, 2021).

2.4.4 Number Distribution

Droplet size distribution depends on the measuring technique employed. The basis of size measuring in the microscopic technique is a number base, while other techniques like the laser diffraction technique are volume base. Mathematical conversation from one basis to another may not yield exact results, as noise will get amplified by a factor of 10^3 for each conversion (Ghobashy *et al*.,2019). Therefore, the results obtained from the present experiment were constructed and presented in a number distribution, which is given as:

$$n_o(x) = \frac{\Delta n_o(x)}{\Delta x} \quad (7)$$

where $n_o(x)$ denotes the average number of droplets per micron range. Integrating equation 7 with respect to particle diameter (x) will provide the total average number of particles size.
This is given by the equation:

$$\int_{X_{min}}^{X_{max}} n(x)\,\Delta x = 1 \quad (8)$$

2.5 Characteristics and Properties of the System

This section provides detailed information on some of the characters and properties of the system

Table 1: High Shear Mixer (Type 18/10) Specifications

Volume	from 1-100 ml
Material	stainless steel
Diameter of the rotor	7.6 mm
Stator diameter	10 mm
Dispersing Gap	0.35 mm
Rotor speed range	2000-20,000 rpm
Viscosity range	up to 5000 MPa.
Process type	Batch
Noise without element	75 dB (A)

DOI: https://doi.org/10.57233/ijsgs.v10i2.664 ISSNp: 2488-9229; ISSNe: 3027-1118
IJSGS FUGUSAU VOL10 (2) WEBSITE: https://fugus-ijsgs.com.ng

Voltage	220V
Power rating input/output	500W/300W
Shaft length	108 mm
Frequency	50/60 Hz

Table 2: Performance Features of Various Dispersion Devices (Gallasi et al., 2019).

Types of devices	Energy dissipation rate (m^2/s^2)	Typical size range (μm)
Static mixers	10-100	50-1000
Agitated vessels	0.1-100	20-500
High shear mixers	1000-100,000	0.5-100
Valve homogenizers	$\sim 10^8$	0.5-1
Ultrasonic	$\sim 10^9$	0.2-0.5

From Table 2, the shear mixer used for the current work falls within the range of 1000 to 100,000 (for energy dissipation rate and typical size ranging from 0.5 to 100 microns. Previous studies have shown that the minimum particle size achievable using the high-energy approach depends on homogenizer type, homogenizer operating conditions (e.g., energy intensity, time, and temperature), sample composition (e.g., oil type, emulsifier type, and relative concentrations), and the physicochemical properties of the component phases (e.g., interfacial tension and viscosity) (Gallasi *et al*., 2019).

2.6 Rate of Shear

According to (Gallasi *et al*., 2019) and (Lebaz *et al*., 2021), the speed of the rotor tip can be calculated from the equation given as:

$$V_{tip} = \pi N d_{rotor} \quad (9)$$

where, N = the number of revolutions of the rotor per second.

The equation for calculating the nominal shear rate is: $\tau = {}^{\pi N d_{rotor}}/_{h}$ (10)

.

The Speed of the rotor depends on the dispersion element used, the viscosity of the medium, and its volume.

Table 3: Properties of the Fluid Sample Used

Fluid	Kinematic Viscosity (cSt)	Relative Density(g/cm^3)	Dynamic viscosity (cP)	Volume Fraction (%)
Distilled water	1.00 @ 20℃	1.00	1.00	70
Pennine Gear oil SEA 90	189 @ 20℃	0.88	166.32	30
Pennine HD Gear oil EP 680	680 @ 20℃	0.95	646.00	30
Pennine HD Gear Oil EP 1500	1500 @ 20℃	0.96	1440.00	30

From Table 2, Pennine Gear oil SEA 90, having specific gravity and viscosity close to that of a light crude oil 35.6 degree API, Heavy duty Gear oil EP 680 with specific gravity and viscosity close to that of a heavy crude oil 22.3 degree API, and extra heavy gear oil EP 1500 were selected for the present experiment. A viscometer was used for measuring the viscosity of the fluids. The temperature of the fluid was measured using a hot plate and calibrating thermometer. According to ASTM D 1250-04 standard, the temperature is a reference point for practical purposes. Since water has its highest density at that point, relative to crude oil and petroleum products. The comparison for the specific gravity of the oil was made from the equation given as:

$$S.G = \frac{141.5}{(API+131.5)} \quad (11)$$

Absolute viscosity (dynamic viscosity) was calculated from the equation given:

$$\text{Dynamic viscosity} = \text{kinematic viscos ity} \times \text{relative density } (S.G) \quad (12)$$

DOI: https://doi.org/10.57233/ijsgs.v10i2.664 ISSNp: 2488-9229; ISSNe: 3027-1118

IJSGS FUGUSAU VOL10 (2) WEBSITE: https://fugus-ijsgs.com.ng

3.0 RESULTS AND DISCUSSION

Oil droplet sizes were measured experimentally using relevant mathematical equations. This chapter presents the results obtained from the experiment and provides a detailed discussion as well. Results were also compared with relevant sources from the literature.

Table 4: Results of the Experiment

Emulsion Samples	Rotor speed N ($rev\ s^{-1}$)	velocity of the rotor tip (ms^{-1})	Share rate (s^{-1})	Droplets size (μm) for SEA 90	Droplets size (μm) for HD EP 680	Droplets size (μm)for HD EP 1500
BATCH 1	33	0.79	2257	105.23	78.00	26.31
BATCH 2	67	1.59	4542	96.00	52.63	17.54
BATCH 3	100	2.38	6800	84.21	31.58	13.16
BATCH 4	133	3.17	9057	42.11	21.05	10.53
BATCH 5	167	3.98	11,371	38.40	15.78	9.25
BATCH 6	200	4.77	13,628	31.58	13.00	8.66
BATCH 7	233	5.56	15,885	21.05	10.53	7.52
BATCH 8	267	6.37	18,200	13.16	8.66	7.28
BATCH 9	300	7.16	20,457	10.52	5.26	5.26
BATCH 10	316	7.54	21,543	8.32	4.21	4.33

Table 4, represents the results of the experiment, containing the characteristic shear rate and the corresponding average droplet size for each emulsion sample that was prepared. The controlling factor for this experiment is the number of revolutions per second (N). The speed of the rotor tip was calculated from Equation 9, and the nominal share rate was obtained from Equation 10. The droplet size provided in this table was estimated on average from the number distribution function from equation 8.

3.1 Shear Effect

The main focus of this section is the anticipated effect of shear on the emulsion droplet size. Referring to Table 4, the results obtained from the experiment show two distinct behaviors. For each emulsion sample, the droplet size decreases with increasing rate of shear and vice versa. This shows a good agreement with the work of Hinze (1955), which states that the maximum droplet size that could exist depends on the rate of energy applied per unit mass. The results obtained by Gallasi *et al*., (2019), show a little variation from the droplet size obtained in this work. This could be a result of the difference in oil viscosity and the stabilizing agents (surfactant) that were used in the previous experiment. The droplet size for each emulsion sample also varies at the same degree of agitation, which is surely due to the difference in viscosity of the emulsions.

One of the limitations of the present experiment is that the present work failed to take account of the rotor speed when the agitating vessel was empty. Studies have shown that the speed of the rotor slightly decreases during the dispersion process, which could possibly be a result of the effect of oil viscosity.

3.2 Viscosity Effect

To investigate the effect of viscosity on droplet size distribution, the current work studied different oil viscosities (189 cSt, 680 cSt, and 1500 cSt) at the same operating conditions. The corresponding droplet sizes for the oil viscosities are compared in Figure 3 below.

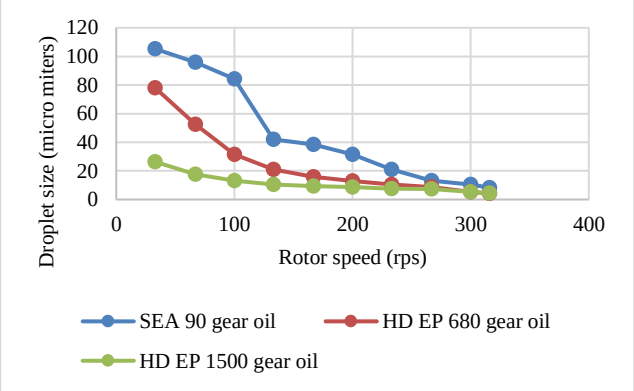

Figure 3: Droplet Size For 3 Different Oil Viscosities at Various Rotor Speed Ranges

From figure 3, the results indicate a reasonable difference between the 3 oil viscosities, which signifies a strong relationship between oil viscosity and droplet size distribution. With the extra heavy oil (1500 cSt) having the least droplet sizes. Gallasi *et al.*, (2019) conducted an experiment with two different oil viscosities. The results show a similar trend to the present work. In this work, the highest viscosity (969 mPa) was also found to be at the lower gradient. This could be a result of the turbulent viscous stress trying to stabilize the oil droplets. Olad *et al.*, (2023) propose that at a high rate of agitation, the emulsification regime changes from turbulent inertia to

turbulent viscous, which results in a reduction in droplet size.

Li *et al.*, (2020), also found that the coalescence rate decreases with increasing oil viscosity, the drainage time between droplets is extended while the collation time remains the same.

4.0 CONCLUSION

The current work conducted an experimental analysis of some of the major factors affecting the rate of coalescence and break-up in oil-water separation and reviews some important mathematical equations that are useful for the engineering design of oil-water separators. The current investigation also reveals that tight emulsions are formed because of high oil viscosity, making the separation of oil-water emulsion harder. The droplet's size range for the three different oil viscosities was between 3 to 100 micrometers.

5.0 RECOMMENDATIONS

The limitation of the present work leads to the following recommendations.

Future research should concentrate on determining the effect of shear on an actual production facility. Model the separation of oil-water, to determine the settling time for different oil viscosities at various realistic shear rates. And also try to investigate the effect of dispersed phase volumetric fraction as well the effect of temperature on oil-water emulsions.

REFERENCES

Al-Kayiem, H. H., Hamza, J. E., & Al-Azawiey, S. S. (2022). Droplet shear in oil/water emulsion produced by centrifugal pump and gear pump. *International Journal of Energy Production and Management. 2022. Vol. 7. Iss. 3*, *7*(3), 193-206. http://dx.doi.org/10.2495/EQ-V7-N3-207-225

Allen, T. (2003). Powder sampling and particle size determination. Elsevier.

Clearaco (2015) Silicon Oil Data Sheet [online] available from <www.clearaco.com> []

Dhandhi, Y., Chaudhari, R. K., & Naiya, T. K. (2022). Development in separation of oilfield emulsion toward green technology–A comprehensive review. Separation Science and Technology, 57(10), 1642-1668. https://doi.org/10.1080/01496395.2021.1995427

Dong, Y., Zhu, C., Ma, Y., & Fu, T. (2022). Distribution of liquid-liquid two-phase flow and droplet dynamics in asymmetric parallel microchannels. Chemical Engineering Journal, 441, 136027. https://doi.org/10.1016/j.cej.2022.136027

Eggers, J., Kempkes, M., & Mazzotti, M. (2008). Measurement of size and shape distributions of particles through image analysis. Chemical Engineering Science, 63(22), 5513-5521. https://doi.org/10.1016/j.ces.2008.08.007

Elger, D. F., LeBret, B. A., Williams, B. C., Crowe, C. T., & Roberson, J. A. (2022). Engineering Fluid Mechanics, International Adaptation. John Wiley & Sons.

Engineering edge Kinetic Viscosity Table Charts of Liquids [online] available from <www.engineeringedge.com/fluid_flow/kinetic-viscosity-table.htm> []

Gallassi, M., Gonçalves, G. F., Botti, T. C., Moura, M. J., Carneiro, J. N., & Carvalho, M. S. (2019). Numerical and experimental evaluation of droplet breakage of O/W emulsions in rotor-stator mixers. Chemical Engineering Science, 204, 270-286. https://doi.org/10.1016/j.ces.2019.04.011

Ghobashy, M. M., Elkodous, M. A., Shabaka, S. H., Younis, S. A., Alshangiti, D. M., Madani, M., ... & El-Sayyad, G. S. (2021). An overview of methods for production and detection of silver nanoparticles, with emphasis on their fate and toxicological effects on human, soil, and aquatic environment. Nanotechnology Reviews, 10(1), 954-977. https://doi.org/10.1515/ntrev-2021-0066

Goodarzi, F., & Zendehboudi, S. (2019). A comprehensive review on emulsions and emulsion stability in chemical and energy industries. The Canadian Journal of Chemical Engineering, 97(1), 281-309. https://doi.org/10.1002/cjce.23336

Hinze, J. O. (1955). Fundamentals of the hydrodynamic mechanism of splitting in dispersion processes. AIChE journal, 1(3), 289-295.

Lebaz, N., Azizi, F., & Sheibat-Othman, N. (2021). Modeling droplet breakage in continuous emulsification using static mixers in the framework of the entire spectrum of turbulent energy. Industrial & Engineering Chemistry Research, 61(1), 541-553. https://doi.org/10.1021/acs.iecr.1c03529

Li, Z., Xu, D., Yuan, Y., Wu, H., Hou, J., Kang, W., & Bai, B. (2020). Advances of spontaneous emulsification and its important applications in enhanced oil recovery process. Advances in colloid and interface science, 277, 102119. https://doi.org/10.1016/j.cis.2020.102119

Liu, Y., Lu, H., Li, Y., Xu, H., Pan, Z., Dai, P., ... & Yang, Q. (2021). A review of treatment technologies for produced water in offshore oil and gas fields. Science of the Total Environment, 775, 145485. https://doi.org/10.1016/j.scitotenv.2021.145485

Murphy, D. B. (2002) Fundamentals of Light Microscopy and Electronic Imaging: John Wiley & Sons

Musgrove, m. (1996) Analysis of Drop Size in liquid/liquid Dispersion at 0.29 Scale for various T/2 IMPELLERS: FMP REPORT 1102

Mutsch, B., Preiss, F. J., Dagenbach, T., Karbstein, H. P., & Kähler, C. J. (2021). Scaling of droplet breakup in high-pressure homogenizer orifices. Part ii: Visualization of the turbulent droplet breakup. ChemEngineering, 5(2), 31. https://doi.org/10.3390/chemengineering5020031

Olad, P., Innings, F., & Håkansson, A. (2023). Turbulent drop breakup in a simplified high-pressure homogenizer geometry: A comparison of experimental high-speed visualization and numerical experiments based on DNS and interface tracking. Chemical Engineering Science, 282, 119274. https://doi.org/10.1016/j.ces.2023.119274

Pun, K., Hamad, F., Ahmed, T., Ugwu, J., Najim, S., Eyers, J., ... & Russell, P. (2023). Experimental investigation of the parameters that affect droplet size and distribution for design calculations of two-phase separators. Heliyon, 9(4). https://doi.org/10.1016/j.heliyon.2023.e15397

Walsh, J. M. (2016). The Savvy Separator Series: Part 5. The Effect of Shear on Produced Water Treatment'. Oil and Gas Facilities 5 (01), 16-23 https://doi.org/10.2118/0216-0016-OGF